The Astrophysical Journal Letters, 889:L26 (5pp), 2020 January 20 https://doi.org/10.3847/2041-8213/ab65bf
© 2020. The Author(s). Published by IOP Publishing Ltd on behalf of the American Astronomical Society.
OPEN ACCESS

The Bipolar Magnetic Emergence in the Solar Polar Region

Chunlan Jin[1], Guiping Zhou[1], Yuzong Zhang[1], and Jingxiu Wang[1,2]
[1] Key Laboratory of Solar Activity, National Astronomical Observatories, Chinese Academy of Science, Beijing 100101, People's Republic of China
cljin@nao.cas.cn
[2] School of Astronomy and Space Science, University of Chinese Academy of Sciences, 100049, Beijing, People's Republic of China
Received 2019 October 28; revised 2019 December 11; accepted 2019 December 18; published 2020 January 24

Abstract

Due to projection effect and polarization sensitivity, it is still unknown whether the bipolar magnetic emergence (BME) exists in the solar polar region. In this study, combining the magnetic observations from the Helioseismic and Magnetic Imager and imaging observations of the 211 Å waveband from the Atmospheric Imaging Assembly, we try to identify and diagnose the BME. Considering the magnetic evolution and the corresponding intensity variation in the extreme ultraviolet waveband, we find definite events of the BMEs in the solar polar region. In total, we identify more than 300 BMEs in the solar polar region in the whole year from 2010 June to 2011 May. We find that whether on the southern or northern polar region, the leading polarity of the BMEs is almost half-positive and half-negative, and the BMEs' magnetic axes show random distribution in that direction. These results imply the possible existence of local dynamo in the solar polar region.

Unified Astronomy Thesaurus concepts: Solar magnetic fields (1503); Sunspots (1653); Solar activity (1475); Solar photosphere (1518); Solar dynamo (2001)

1. Introduction

Observation of the magnetic field in the solar polar region is very important to understand the long-term variation and the origin of solar magnetism. It also holds the key to understand the origin of solar wind and coronal heating. Concentration of the flux in the polar region is predominantly unipolar with a mean field of several Gauss (Babcock & Babcock 1955; Babcock 1959; Svalgaard et al. 1978; Tsuneta et al. 2008). Away from solar minimum, the magnetic flux of the decaying active region (AR) migrates poleward, which makes the dominant polarity of the polar field reverse near the solar maximum (Babcock 1959). The source of the magnetic field in the polar region has been explained by the current solar global dynamo models (Wang et al. 1991; Sheeley 1992, 2005; Choudhuri et al. 1995; Jiang et al. 2014): magnetic flux produced by midlatitude bipolar AR emergence is dispersed into the polar region owing to differential rotation, meridional flow, and turbulent diffusion.

However, more and more observations have challenged the solar global dynamo models to explain the magnetic origin in the solar polar region. The polar field may appear as unipolar in low-resolution magnetograms, but in fact it is dominated by small-scale magnetic elements of mixed polarities (Severny 1971). Based on the high-resolution magnetograms of Big Bear Solar Observatory, Lin et al. (1994) confirmed that the solar polar regions are concentrated with small-scale magnetic elements of both polarities. That is to say, in the Sun's polar regions, not only the field of dominant polarity, but also the field with a opposite polarity is always present (Lin et al. 1994; Obridko et al. 2014), and the flux ratio between them even reaches 1/2 (Tsuneta et al. 2008; Jin & Wang 2011). Lin et al. (1994) estimated the field strength of magnetic elements in the solar polar region and found that the average magnetic field strength of the dominant polarity increases as the solar cycle evolves toward the sunspot minimum. Meanwhile, the average field strength of the nondominant polarity decreases. Using the observations from the Michelson Doppler Imager on board the *Solar and Heliosphere Observatory*, Benevolenskaya (2004) revealed that the total polar magnetic flux does not vary significantly during the polar magnetic field reversals in both hemispheres, while the positive and negative components of the total flux do change. Shiota et al. (2012) indicated that the magnetic concentrations of the vertical magnetic fields in the polar region consist of two different components based on the observation from the Spectro-Polarimeter of Solar Optical Telescope on board *Hinode*: one corresponds to the large-scale flux concentrations with a dominant polarity, whose flux varies with the solar cycle; the other is composed of the small-scale flux concentration of both polarities, whose flux does not vary with the solar cycle.

However, the fact is that the line-of-sight (LOS) field observed in the polar region mainly corresponds to the horizontal field in the local frame. It is difficult to decide the polarity of magnetic field observed in the polar region due to the severe projection effect and polarization sensitivity. Here, we study the bipolar magnetic emergence (BME) in the polar region. A suggestion is that if the magnetic field originates from the diffusion of the decaying AR, the magnetic nature in the polar region will obey the magnetic law of AR produced by the global dynamo. BMEs are identified in the polar region by combining the magnetic observation and the corresponding extreme ultraviolet image observation. We discuss whether the small-scale field like BME obeys AR magnetic law, and then explore the possibility of local dynamo in solar polar region. The observations from the Helioseismic and Magnetic Imager (HMI; Scherrer et al. 2012; Schou et al. 2012) and the Atmospheric Imaging Assembly (AIA; Lemen et al. 2012) are used in this study. The Letter is organized as follows. Section 2 is devoted to observations and data analysis. Section 3 presents the identification of BMEs in the polar region. Section 4 presents the concluding remarks.

Original content from this work may be used under the terms of the Creative Commons Attribution 4.0 licence. Any further distribution of this work must maintain attribution to the author(s) and the title of the work, journal citation and DOI.

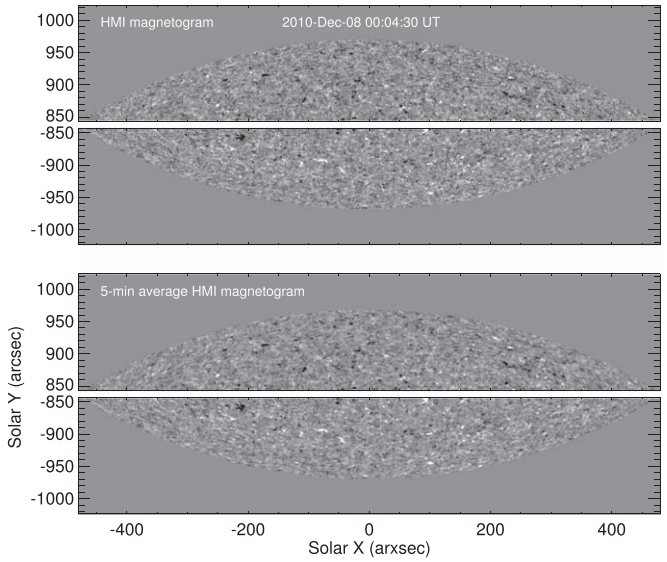

Figure 1. Observed HMI magnetogram and the corresponding 5 minute average magnetogram in the solar polar region. The magnetograms saturate at ±30 G.

2. Observations and Data Analysis

In this study, one set of HMI LOS magnetograms with a cadence of 45 s is selected from 2010 June to 2011 May. The corresponding AIA images at 211 Å are coaligned with the magnetic observations. We use the data in the field of view within a 0.995 disk radius and the altitude higher than 60° from the line connecting the easternmost and westernmost edges of the Sun.

In order to improve the signal-to-noise level, seven continuous magnetograms in an interval of 5 minutes are averaged to create a 5 minute average magnetogram. A comparative sample of the 5 minute average magnetogram and the 45 s magnetogram is shown in Figure 1, and more magnetic signals can be found in the 5 minute average magnetogram. Then based on these 5 minute average magnetograms, we analyze the variation of the LOS magnetic field from solar disk center to solar limb, which is shown in the right panel of Figure 2. It can be found that the LOS field weakly decreases far away from the solar disk center. Therefore, the radial-field assumption of the field vector is not adopted in this study, although it has been widely used in data analysis (Svalgaard et al. 1978; Wang & Sheeley 1992). Following the method used for estimating noise level (Hagenaar 2001; Liu et al. 2004; Jin et al. 2011), we analyze the histogram of the magnetic field of each pixel in the polar region, and assume that the magnetic field has a Gaussian distribution. Finally, the distribution of low-field pixels is fitted by a Gaussian function, and the half-width of the Gaussian function is defined as 1σ, which is shown in the left panel of Figure 2. In this study, the threshold of 2σ (i.e., 8 G) is adopted to extract magnetic signals.

3. The Identification of BMEs in the Polar Region

As referred to before, BMEs in the polar region are explored with simultaneous AIA and HMI observations. Two criteria are applied to identify BMEs in the polar region based on the observations. First, a pair of emerging fluxes with opposite polarities in the LOS magnetograms is observed quasi-instantaneously in the solar surface, and grows up simultaneously in both area and absolute flux magnitude. Second, the EUV loops connecting the opposite polarities appear and will be lightened with the increasing magnetic flux.

We definitely find the BME events in this period from 2010 June to 2011 May. An example of the identified BME is illustrated in Figure 3. The BME is observed in the southern pole of the Sun on 2011 May 12. At 07:29 UT, the two polarities of the BME begin to emerge on the solar surface, and gradually grow up and separate from each other. With the evolution, the BME has a maximum flux with a value of 2.2×10^{19} Mx at 11:29 UT. At about 17:59 UT, the bipoles are mostly separated, and then begin to approach gradually and cancel. Finally, the flux of the positive polarity disappears at about 10:00 UT the next day. The EUV brightening loop structure always connects the BME during its evolution.

Another example of the identified BME is displayed in Figure 4. The BME appears in northern pole on 2010 November 22. At about 22:00 UT, the negative polarity of the BME appears half an hour later than the positive polarity. Then their flux gradually merges with the surrounding existing magnetic field, separately. With the magnetic evolution, the bipole increases in the magnetic flux and gradually separates. At about 15:00 UT in the next day, the separation of the two poles reaches maximum, and then the bipoles begin to gradually approach each other until one disappears. The EUV brightening loop structure and the BME appear almost simultaneously, and the loop structure accompanies the BME from its birth to death.

The BMEs in the solar polar region are identified and tracked in the aspect of the evolution based on the magnetograms and AIA data. In total, 166 BMEs in the northern polar region and 154 BMEs in the southern one are definitely identified. According to the Hale's polarity rule of solar activity: for the great majority of large ARs during one sunspot cycle, their leading polarities on the northern hemisphere have the same sign, which is opposite to that on the southern hemisphere. In this study, we determine the gravity center positions of both polarities for each BME. We find that the leading polarity of the BMEs on the northern polar region does not display a dominant sign: 48% are positive, and 52% are negative; while on the southern polar region, the leading polarity of the BMEs does not have the same sign either: 56% negative polarity and 44% positive one. Further, we obtain the tilt direction of the BME magnetic axis. We show the position and direction distributions of these BMEs, which are shown in Figure 5. In order to display the results better, we use the same length to show the direction distribution of these magnetic axes in a concentric circle, which is shown in the top left and bottom left of Figure 5. Unlike what was described by Joy's law of solar activity, i.e., the closer-to-equator of the leading polarity in ARs than that of the trailing polarity, the BME orientation shows almost a random distribution whether on the southern or northern polar region. Figure 6 shows the graphics of BME orientation distribution for the northern and southern polar regions, respectively. It can be found that there is a preponderance for east–west and west–east bipole emergence. The fact of having few north–south and south–north bipole emergence is probably caused by the severe projection effect in the polar region. The figure shows that the BME orientation is

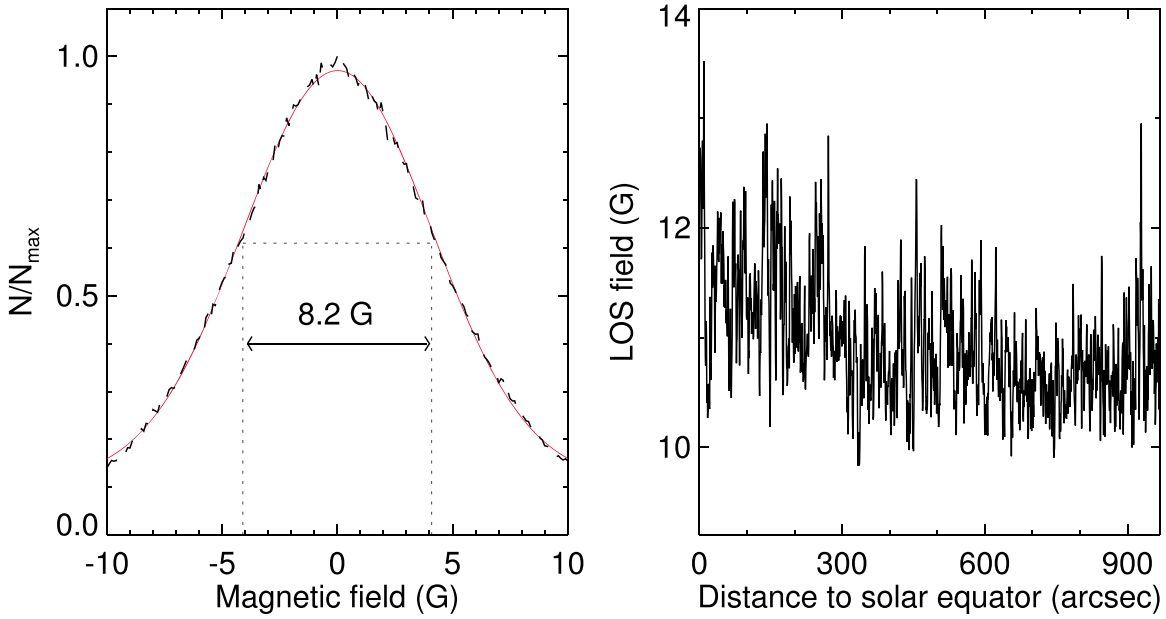

Figure 2. Left panel: the distribution of low-field pixels in the solar polar region (black line) and the corresponding Gaussian fitting (red line). Right panel: the variation of the LOS field from solar disk center to solar limb.

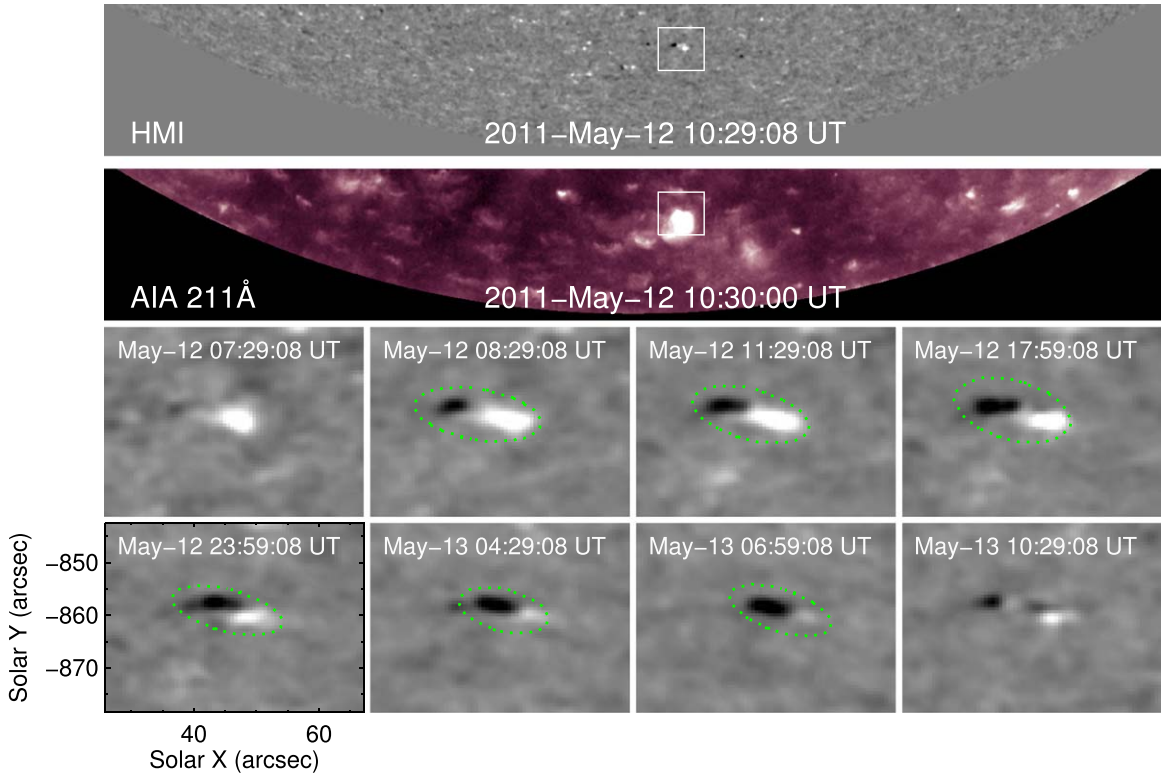

Figure 3. Example of the identified BMEs based on the HMI magnetic observations and AIA images at 211 Å. The BME is located in the southern pole, which is indicated by the white box in the top two panels. The bottom two rows show the magnetic evolution of BME from its appearance to disappearance in the field of view of the white box. The BMEs are highlighted by the green dotted ellipses. The brightening at 211 Å is shown in the second row.

different from that of AR, and it is inconspicuous compared with 95% of ARs having a proper orientation (Harvey 1993).

4. Concluding Remarks

Based on the observations from the HMI magnetogram and AIA imaging observations at the 211 Å waveband, we definitely find the BME events in the solar polar region. Moreover, more than 300 BMEs in this period from 2010 June to 2011 May are identified: 166 BMEs in the northern polar region and 154 BMEs in the southern polar region. We definitively track them from their early emergence to final disappearance, and find that they contribute the magnetic flux of 10^{19} Mx every day to the surface of the polar region. In

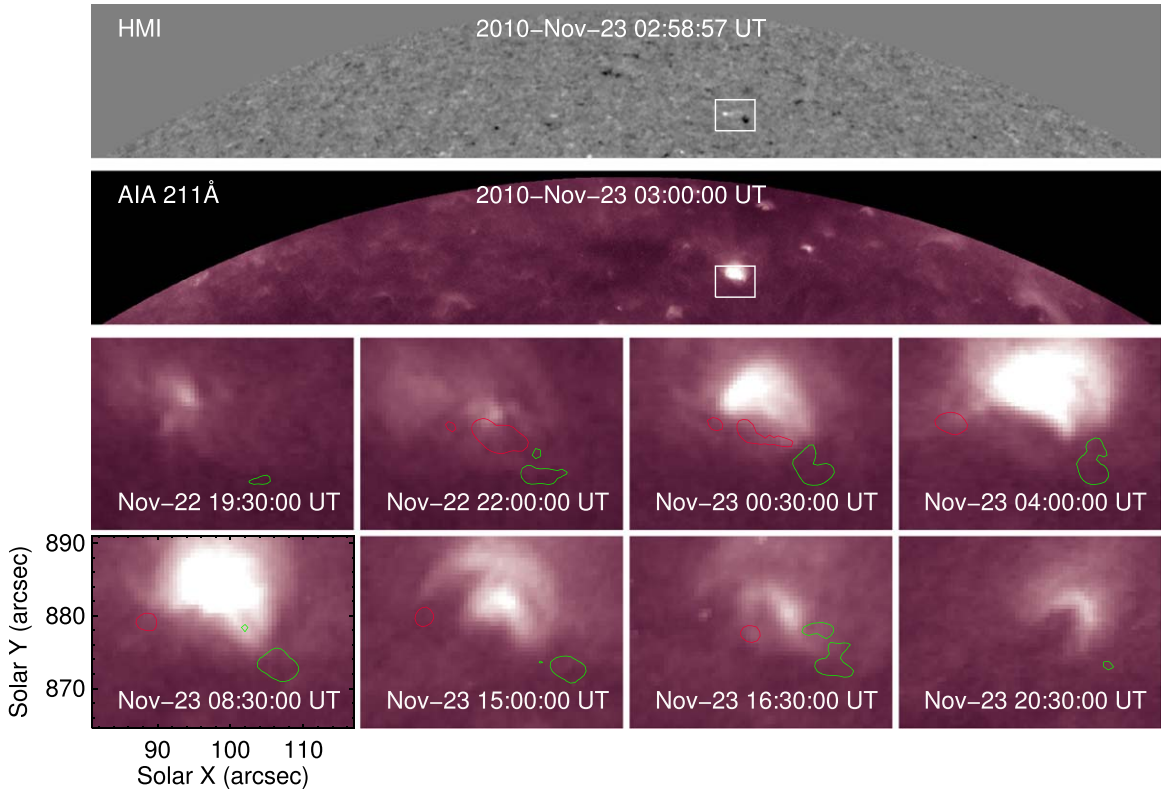

Figure 4. Another example of an identified BME. Similar to Figure 3, the top two panels display the BME on the images from the HMI and AIA at 211 Å waveband. The bottom eight panels show the variation of EUV intensity at the 211 Å waveband during the BME evolution, and the red and the green lines mean the contours of 30 G for the positive and negative magnetic field, respectively.

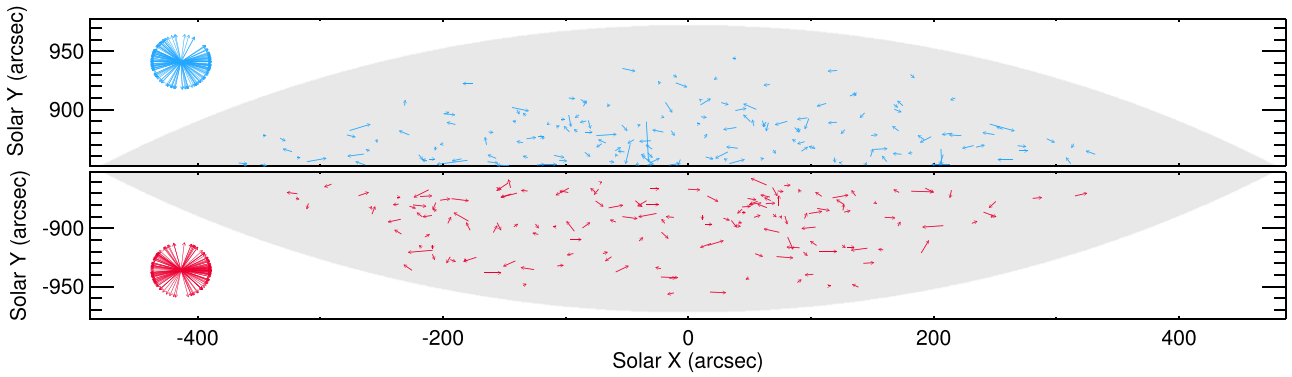

Figure 5. Direction distribution of magnetic axis for these BMEs in the southern and northern polar regions. Each arrow starts from the magnetic barycenter of the positive polarity of the corresponding BME. The blue arrows in the top left corner and the red arrows in the bottom left mean the distributions of tilt direction for BMEs in a concentric circle in the corresponding polar region.

addition, 52% of the identified BMEs in the northern polar region are found to have the same orientation as AR, while in the southern polar region less than half the BMEs have the proper orientation. Harvey (1993) states that, as the cycle activity wanes, the tendency for bipoles to have the same orientation as ARs decreases. Considering the fact that solar cycle 24 is a weak cycle and the observations in this study are taken during the solar minimum of cycle 24, our result is in agreement with Harvey (1993) (i.e., 56% of bipoles having a proper orientation) and Hagenaar (2001) (i.e., 60% of bipoles having a proper orientation). According to Joy's law, the trailing polarity of a bipolar AR should be located poleward of the leading polarity. However, the trailing polarity of these BMEs is not preferentially located compared with their leading polarity whether on the southern or northern polar region, i.e., a random distribution.

These BMEs can be classified as ephemeral regions in nature (Wang et al. 2012), which are emerged locally in the polar region and clearly not the manifestation of the transported toroidal flux from the Sun's activity belt. They are likely to be from the products of the local dynamo operation. The result confirms the possible existence of a local dynamo in the solar polar region along with the global dynamo.

In addition, the number of identified BMEs could be a low limit of BMEs in the solar polar region. The interaction of the small-scale BME field originated from the local dynamo and

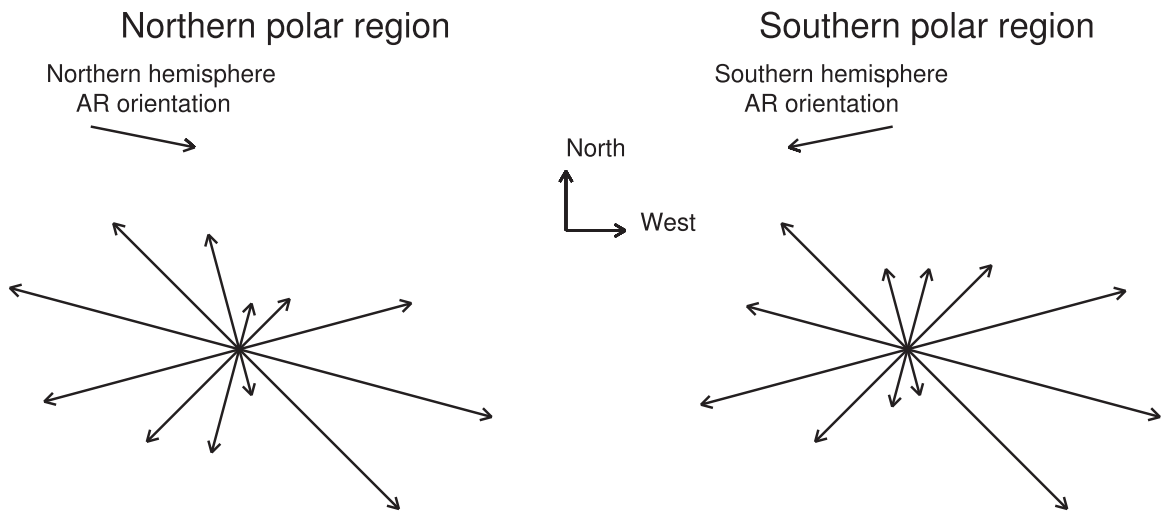

Figure 6. Graphics of BMEs orientation distribution in the southern and northern polar regions. The length of an arrow is proportional to the number of BMEs that are oriented in that direction. The proper direction of AR in each hemisphere is also displayed.

the field of dominated polarity from global dynamos may play a very important role in coronal heating and solar wind accelerating (Tu et al. 2005). More careful and serious efforts need to be made to further explore this possibility.

The work is supported by the National Natural Science Foundation of China (11533008, 11573038, and 11873059) and Basic Frontier Scientific Research Programs of CAS (ZDBS-LY-SLH013).

ORCID iDs

Chunlan Jin https://orcid.org/0000-0003-4763-0854
Guiping Zhou https://orcid.org/0000-0001-8228-565X
Jingxiu Wang https://orcid.org/0000-0003-2544-9544

References

Babcock, H. D. 1959, ApJ, 130, 364
Babcock, H. W., & Babcock, H. D. 1955, ApJ, 121, 349
Benevolenskaya, E. E. 2004, A&A, 428, L5
Choudhuri, A. R., Schussler, M., & Dikpati, M. 1995, A&A, 303, L29
Hagenaar, H. J. 2001, ApJ, 555, 448
Harvey, K. L. 1993, Magnetic bipoles on the Sun, PhD thesis, Rijksuniv. Utrecht
Jiang, J., Hathaway, D. H., Cameron, R. H., et al. 2014, SSRv, 186, 491
Jin, C. L., & Wang, J. X. 2011, ApJ, 732, 4
Jin, C. L., Wang, J. X., Song, Q., & Zhao, H. 2011, ApJ, 731, 37
Lemen, J. R., Title, A. M., Akin, D. J., et al. 2012, SoPh, 275, 17
Lin, H., Varsik, J., & Zirin, H. 1994, SoPh, 155, 243
Liu, Y., Zhao, X. P., & Hoeksema, J. T. 2004, SoPh, 219, 39
Obridko, V. N., Chertoprud, V. E., & Kuzanyan, K. M. 2014, SoPh, 289, 2867
Scherrer, P. H., Schou, J., Bush, R. I., et al. 2012, SoPh, 275, 207
Schou, J., Borrero, J. M., Norton, A. A., et al. 2012, SoPh, 275, 327
Severny, A. B. 1971, in IAU Symp. 43, Solar Magnetic Fields, ed. R. Howard (Dordrecht: Reidel), 675
Sheeley, N. R., Jr. 1992, in ASP Conf. Ser. 27, The Solar Cycle, ed. K. L. Harvey (San Francisco, CA: ASP), 1
Sheeley, N. R., Jr. 2005, LRSP, 2, 5
Shiota, D., Tsuneta, S., Shimojo, M., et al. 2012, ApJ, 753, 157
Svalgaard, L., Duvall, T. L., Jr., & Scherrer, P. H. 1978, SoPh, 58, 225
Tsuneta, S., Ichimoto, K., Katsukawa, Y., et al. 2008, ApJ, 688, 1374
Tu, C. Y., Zhou, C., Marsch, E., et al. 2005, Sci, 308, 519
Wang, J. X., Zhou, G. P., Jin, C. L., & Li, H. 2012, SoPh, 278, 299
Wang, Y. M., & Sheeley, N. R., Jr. 1992, ApJ, 392, 310
Wang, Y. M., Sheeley, N. R., Jr., & Nash, A. G. 1991, ApJ, 383, 431